www.dergipark.gov.tr
ISSN:2148-3736

El-Cezerî Journal of Science and Engineering
Vol: 10, No: 2, 2023 (284-295)
DOI: 10.31202/ecjse.1210453

ECJSE

Research Paper

Performance of Tin Oxide Supported on Reduced Graphene Oxide for Oxidative Desulfurization

Qahtan A. MAHMOOD[1a], Basma Abbas ABDULMAJEED[2b]

[1]Tikrit University, College of Engineering, Chemical Engineering Department IRAQ.
[2]Baghdad University, College of Engineering, Chemical Engineering Department, IRAQ.
qahtan.adnan@tu.edu.iq

Received: 26.11.2022 **Accepted:** 11.01.2023

Abstract: In this study, the incipient wetness impregnation (IWI) method was used to prepare tin oxide nanoparticles supported on reduced graphene oxide nanosheets (SnO_2/rGO). Characterize of catalyst composite were analyzed by X-ray diffraction (XRD), Fourier transforms infrared spectroscopy (FTIR), Field emission scanning electron microscope (FESEM), energy dispersive X-ray spectroscopy (EDX), and Raman spectroscopy. The activity of the SnO_2/rGO catalyst was evaluated in the catalytic oxidation process of dibenzothiophene (DBT) for modeled oil and diesel fuel in the presence of H_2O_2 as an oxidant. Optimum reaction conditions (the loading quantity of the tin oxide, the concentration of dibenzothiophene, the time of reaction, the temperature, the amount of oxidant, and the catalyst dosage) were investigated in a batch reactor. High-value of dibenzothiophene (DBT) removal from modeled oil samples was 79.14% at temperature = 60 ◦C, reaction time = 90 min, catalyst dosage = 0.04 g, amount of H_2O_2 = 0.375 mL, and 385 ppm concentration of dibenzothiophene. Catalyst activity at the same operating condition was also investigated for diesel fuel and the removal of sulfur was 35.81%

Keywords: Tin oxides catalyst, rGO support, ODS desulfurization

1. Introduction

With rapid economic development in the world, the consumption of liquid fuels has increased. Sulfur in hydrocarbon-based distillates fuel is the main pollutant. The combustion of sulfur compounds in liquid fuels may release sulfur oxides (SOX) into the atmosphere, causing acid rain and air pollution [1]. Therefore, at present, very strict regulations for low-sulfur fuels are being implemented in oil refineries around the world to reduce the sulfur content in their products to a very low limit of 10-50 ppm [2,3]. Although the technology of hydrodesulfurization from oil products is widely used in industry, it is more expensive due to the fact that it is carried out under harsh operating conditions. In addition, heterocyclic sulfides and their derivatives cannot be removed completely due to resistance at high temperatures. Therefore, alternative desulfurization techniques have been used, such as extraction, bio-desulfurization, adsorption, photooxidation, and oxidation [4,5]. Among these technologies, oxidative desulfurization (ODS) offers advantages such as simplicity, lower cost-effectiveness, and carrying out at middle operating conditions [6].

Molecular oxygen (O_2), hydrogen peroxide (H_2O_2), formic acid (CH_2O_2), and ozone (O_3) are widely used in the selective oxidation of sulfur compounds in the ODS process [7]. Recently, several studies have been conducted to identify the effective use of graphene and its derivative (graphene oxide and reduced graphene oxide) as supports for metals in ODS processes [8]. The use of graphene materials that have many properties such as high surface area, chemical inertness, mechanical robustness, and thermal conductivity as active metallic support has been shown highly important in much oil research lastly [9,10].

How to cite this article
Mahmood Q. A., AbdulMajeed B. A., "Performance of tin oxide supported on reduced graphene oxide for oxidative desulfurization," *El-Cezerî Journal of Science and Engineering*, Vol. 10, No. 1, 2023, pp. 284-295.
ORCID: [a]0000-0002-1476-0401; [b]0000-0002-2610-7872

In this study, the incipient wetness impregnation (IWI) method was used to prepare tin oxide nanoparticles supported on reduced graphene oxide nanosheets (SnO_2/rGO). Characterize of catalyst composite were analyzed by X-ray diffraction (XRD), Fourier transforms infrared spectroscopy (FTIR), Field emission scanning electron microscope (FESEM), energy dispersive X-ray spectroscopy (EDX), and Raman spectroscopy. The activity of the SnO_2/rGO catalyst was evaluated in the catalytic oxidation process of dibenzothiophene (DBT) for modeled oil and diesel fuel in the presence of H_2O_2 as an oxidant. Optimum reaction conditions (the loading quantity of the tin oxide, the concentration of dibenzothiophene, the time of reaction, the temperature, the amount of oxidant, and the catalyst dosage) were investigated in a batch reactor. Finally, the activity of (SnO_2/rGO) catalyst under best-operating conditions was tested for diesel fuel.

2. Experimental

2.1. Chemicals Materials

Chemicals materials used in this study, Dibenzothiophene (DBT), hydrogen peroxide (H_2O_2) 30% (v/v), and stannous chloride dehydrate ($SnCl_2.2H_2O$), were purchased from Sigma-Aldrich, USA. Methanol (CH_3OH) 99% was obtained by Fisher Scientific. (n-heptane) 99% from Sigma Aldrich was used as modeled oil.

2.2. Preparation of SnO2/rGO Composite Catalyst

Reduced graphene oxide (rGO) was synthesized from polyethylene Terephthalate PET waste by a pyrolysis in catalytic reactor. Reduced graphene oxide has heated 80 °C in oven to remove pore moisture of support and to speed up the diffusion of the solute into the pores. Stannous chloride dihydrate ($SnCl_2.2H_2O$) has used as the metal precursor to preparation SnO_2/rGO catalyst. The quantity of the active material of was added to deionized water and the solution was stirred for 60 minutes at room temperature till all Stannous chloride dihydrate dissolved in water[11,12]. Reduced graphene oxide has added to the prepared solution with continuous stirring of the mixture for 120 minutes at room temperature until the mixture is total impregnated. The impregnated SnO_2/rGO catalyst has dried at 100 °C in an oven for 24 hours to eliminate water and crystalize the salt in the pore surface. The dried catalyst has calcined at 400 °C in a furnace for 2 hours with N_2 flow rate to convert the salt to oxides over catalysts support.

2.3. ODS Activity of the Catalyst

The activity of the SnO_2/rGO catalyst for the oxidative desulfurization process was investigated in a batch reactor using H_2O_2 as oxidation. 15 ml of modeled oil (n-heptane) at a concentration of DBT 385ppm was taken in a three-neck flask fitted with a reflux condenser. The flask was placed in a water bath to maintain constant distribution of temperature, under atmospheric pressure. When the reaction is finished, the SnO_2/rGO catalyst was collected by filtration, and the sample was analyzed to find a final concentration of DBT (ppm). Several experiments were conducted under different conditions in order to find the best condition for the ODS process.

2.4. Analyses

DBT concentration in the modeled oil and diesel fuel sample was analyzed by analytik Jena multi EA 5000 – Micro-elemental Analyzer (Germany), DBT conversion was calculated using Equation (1).

$$\text{DBT Removal } \% = \frac{C_o - C_t}{C_o} * 100 \quad (1)$$

3. Results and Discussion

3.1. Characterization of the Catalyst

The X-ray diffraction of rGO and SnO_2/rGO catalysts is depicted in figure 1. XRD pattern of rGO support shows a major peak at 23.06◦, with an interlayer spacing (d) of 0.386 nm. In addition, the calculated crystal size of rGO layer is 4.04 nm. Therefore, rGO crystal has almost fewer layers[13,14]. The rGO peak is observed with the same intensity after Sn is impregnated onto rGO, this means no disruption in rGO crystallinity. All SnO_2/rGO catalysts reflect SnO_2 diffraction peaks at (26.8°, 33.9°, 38.16°, 51.9°, and 65.5°) demonstrating the feasibility of wetness impregnation method to support Sn onto rGO[15].

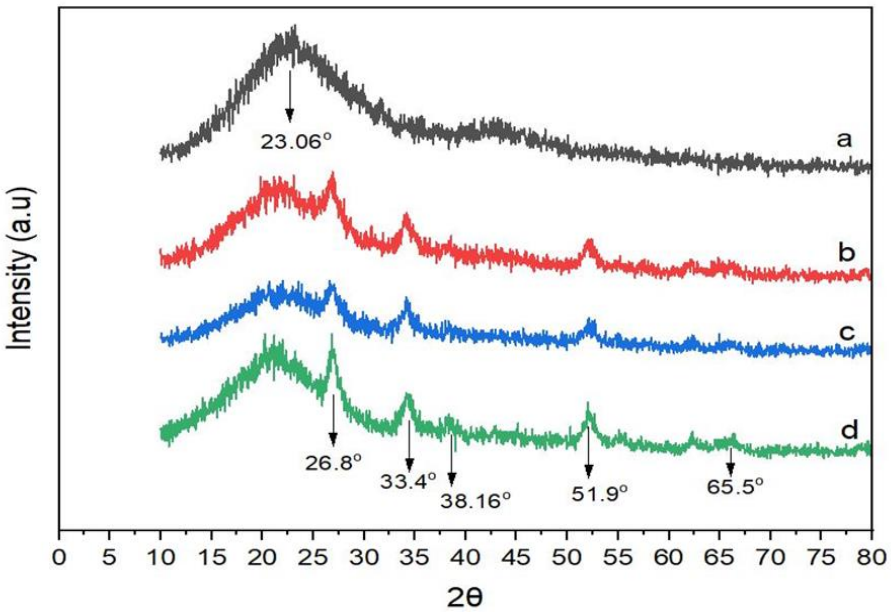

Figure 1. XRD patterns of (a) reduced graphene oxide, (b) 10%SnO_2/rGO, (c)15%SnO_2/rGO, and (d) 20%SnO_2/rGO

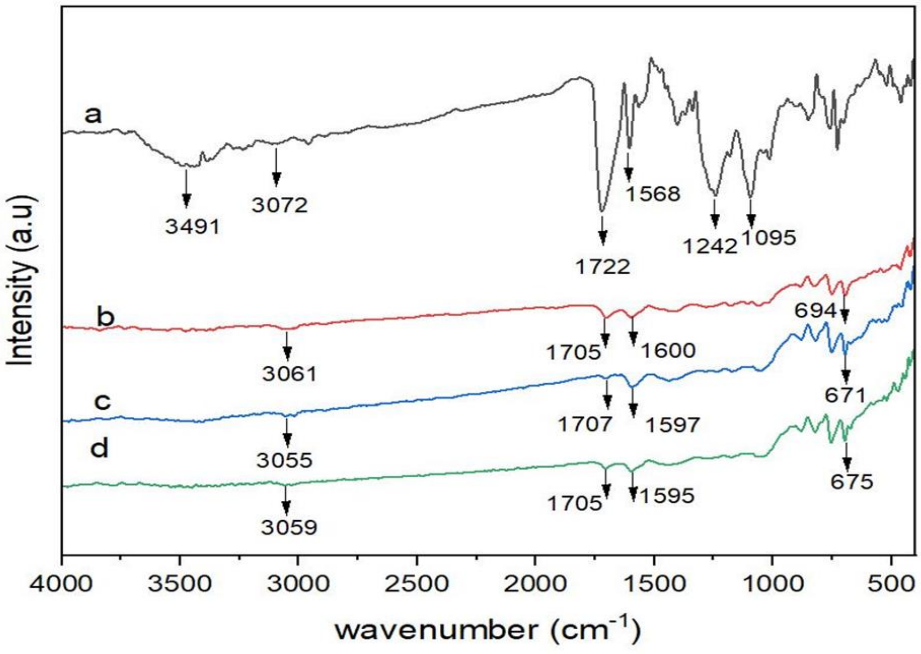

Fig. 2. FTIR spectra of (a) reduced graphene oxide, (b) 10%SnO_2/rGO, (c)15%SnO_2/rGO, and (d) 20%SnO_2/rGO.

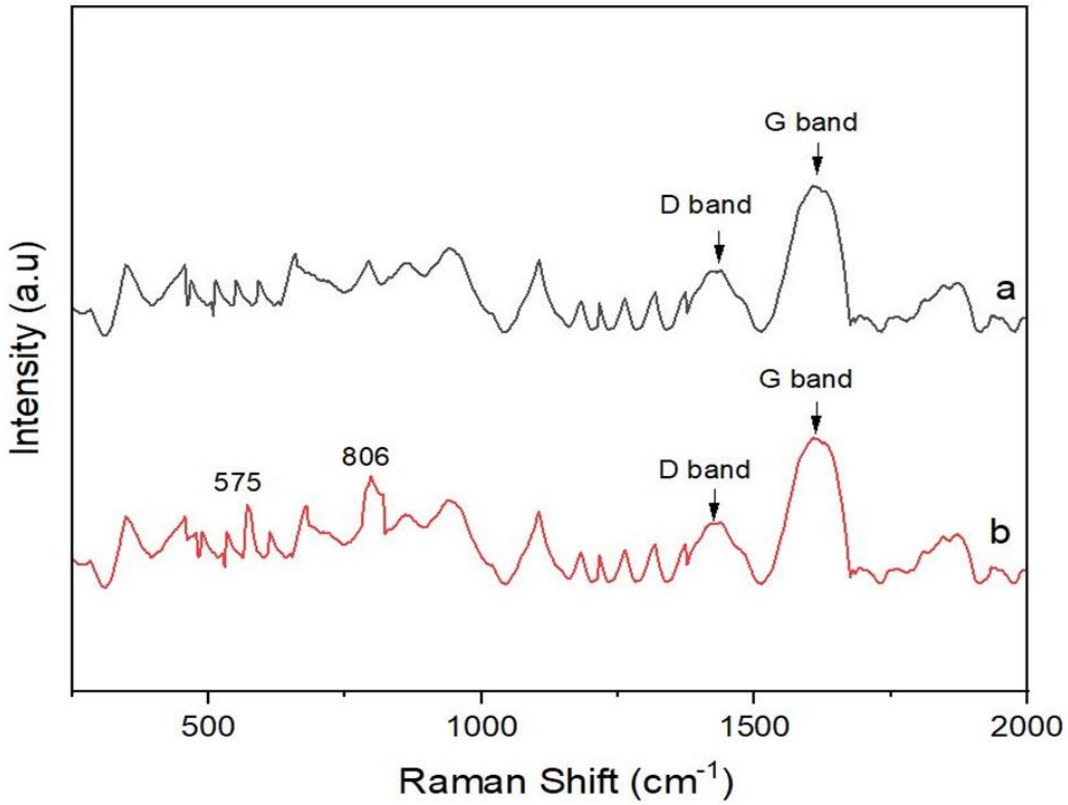

Figure 3. Raman spectra of (a) reduced graphene oxide, (b) 20%SnO_2/rGO

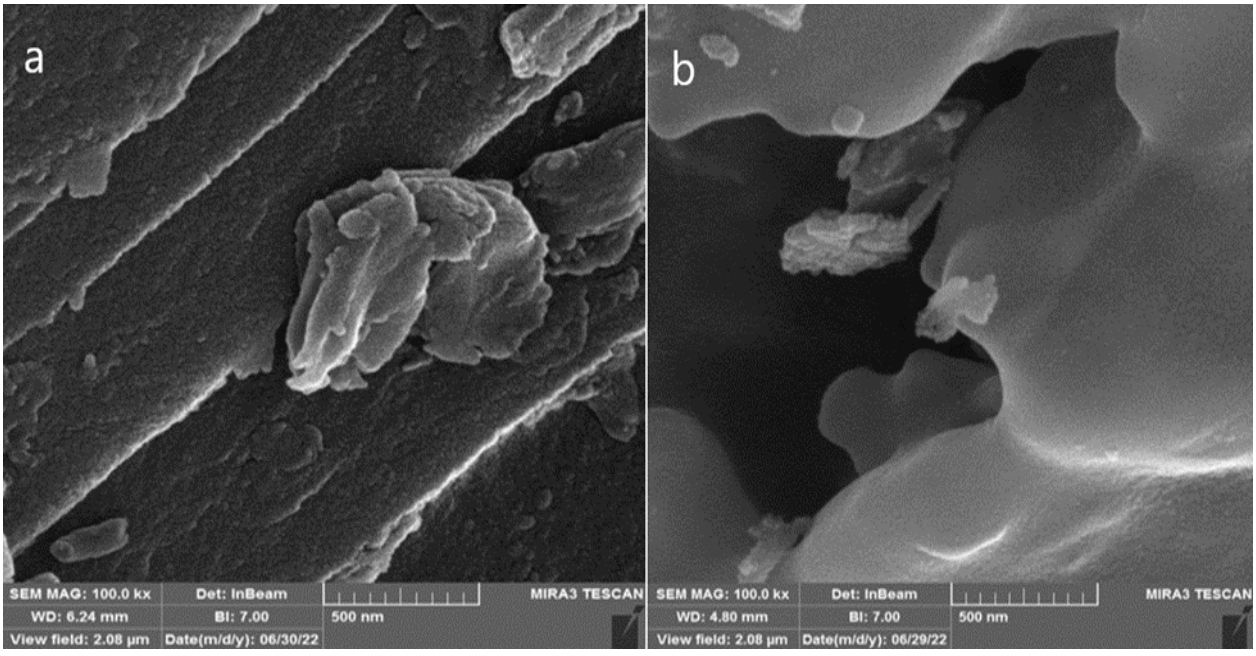

Figure 4. FESEM of (a) reduced graphene oxide, (b) 20%SnO_2/rGO

The FTIR spectra of rGO and SnO2/rGO catalysts is shown in Figure 2. Broad absorption at 3491 $cm^{-1}$and 3072 cm^{-1} are attributed to the O-H stretching vibration in rGO. The peak at 1722 cm^{-1} reflects the vibrational range of carbonyl functional groups (C=O/COOH). the stretching and bending of C-O bonds in carboxyl were observed at the peak of 1558 cm^{-1} , while the peak at 1242 cm^{-1} comes from C = C bonds in carboxyl-groups [16]. The presence of C-O bonds in alkoxy is shown from the

stretching at 1091 cm^{-1}. The SnO_2/rGO spectrum shows new peaks appearing at 650-700 cm^{-1} after metal loading on rGO during the synthesis step [17,18].

Figure 3 displays Raman spectra of rGO and the 20%SnO_2/rGO. From the figure, we see two main peaks (D band) (disordered band) at 1362 cm^{-1} which indicates to present a defect in rGO, and (G band) (graphitic band) at 1606 cm^{-1} which normally assigned the sp2 of carbon atoms[19]. The band centered at 575 and 806 cm^{-1} has been reported for SnO_2 nanoparticles[20].

The FESEM-EDX images of rGO and SnO2/rGO catalysts are shown in Figures 4 and 5 respectively. FESEM image of the rGO with 500 nm microscopy showed that rGO contains multilayered graphene nanosheets [21]. From the EDX mapping, Figure 5, it can be seen that rGO consists of C=73.16 and O = 17.64 with a small content of another element. The high percentage of Sn on the reduced graphene oxide is due to the high Sn content loaded which was 55.28 Wt.%. With increasing Sn content, agglomeration of SnO_2/rGO catalyst can occur as reported in the EDX mapping. Agglomeration has also been demonstrated by the lowest surface area of catalysts [22].

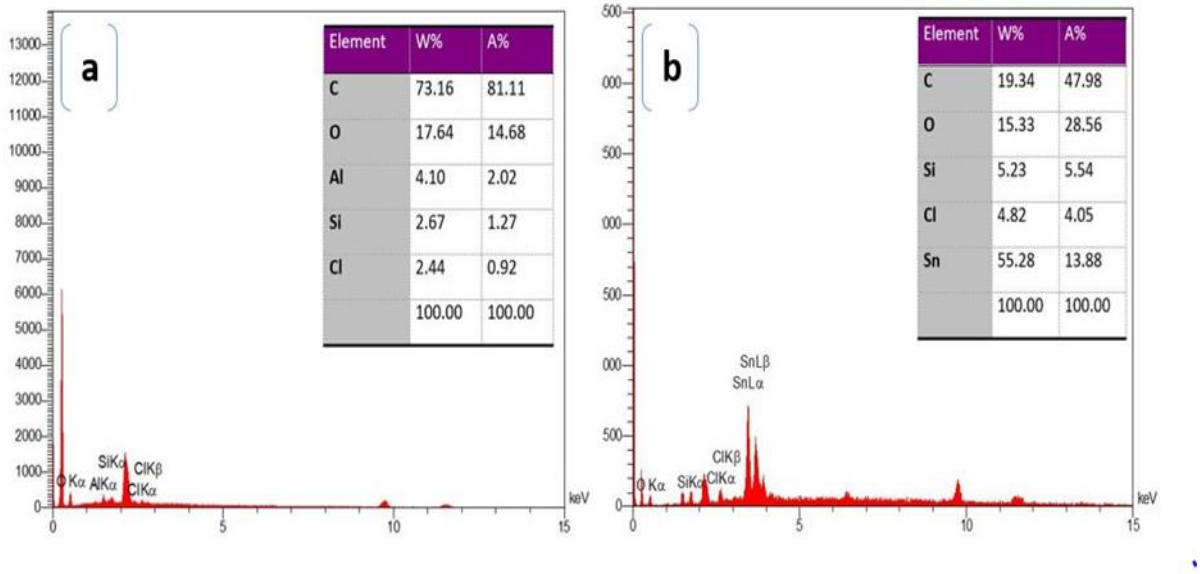

Figure 5. EDX of (a) reduced graphene oxide, (b) 20%SnO_2/rGO

3.1.1 Surface Area of Catalyst

The BET surface area, pore volume, and pore diameter of rGO and SnO_2/rGO were shown in Table 1. From the results, we observed decreases in the surface area of SnO_2/rGO when the tin metal content increased from 10% to 20%.

Table 1. BET surface area, pore volume, and pore diameter of rGO and SnO_2/rGO

Sample	SBET (m2/g)	VP (cm3/g) nm	D (nm)
rGO	31.04	0.038	4.87
10%SnO_2/rGO	13.60	0.04	12.36
15%SnO_2/rGO	12.89	0.039	12.12
20%SnO_2/rGO	12.07	0.04	13.40

3.2. ODS Activity of SnO_2/rGO

The SnO_2/rGO catalyst activity for ODS was investigated using n- heptane as a modeled oil sample and H_2O_2 as oxidant. Removal of DBT was examined under different conditions of reaction time, initial concentration of DBT, temperature of reaction, catalyst dosage, and amount of oxidant.

3.2.1. Effect of Time of Reaction

The oxidation of DBT was carried out at different reaction times (45-180 min) and DBT concentrations ranging from (385 to 933 ppm). In contrast, other experimental conditions, such as catalyst dosage (0.02 g), reaction temperature (50 ◦C), and amount of oxidant (0.25 ml) were kept constant.

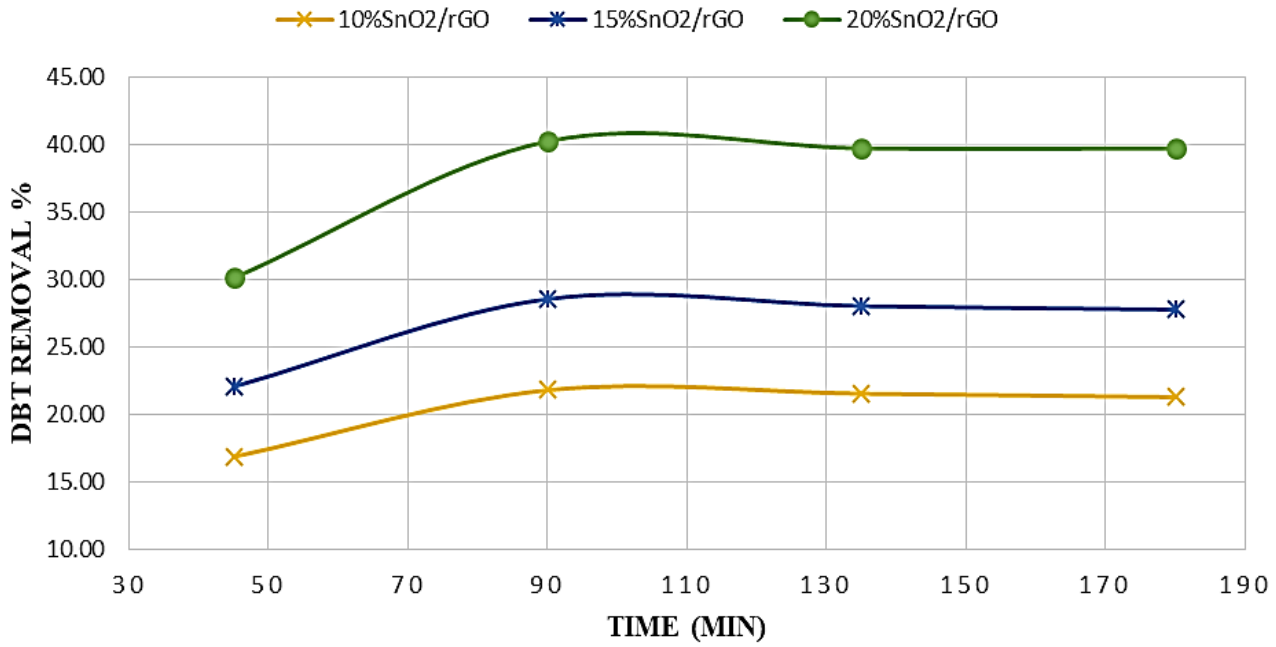

Figure 6. Comparison of the activities of the catalysts at concentration of dibenzothiophene 385 ppm [Reaction conditions: T = 50 °C, Cat. dos = 0.02 g, and amount of oxidant =0.25 ml].

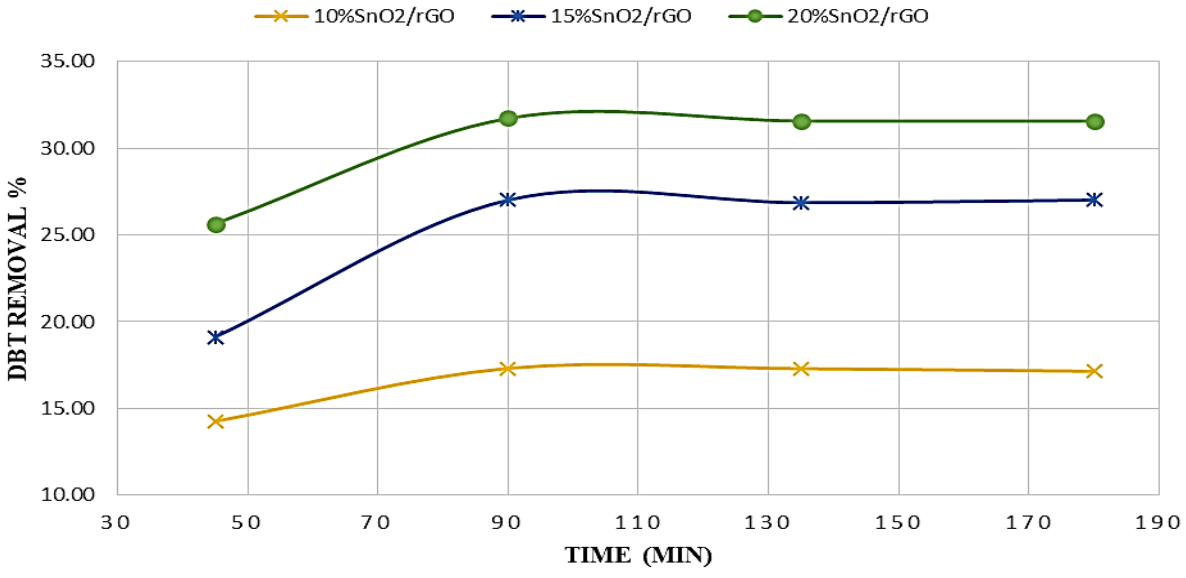

Figure 7. Comparison of the activities of the catalysts at concentration of dibenzothiophene 659 ppm [Reaction conditions: T = 50 °C, Cat. dos = 0.02 g, and amount of oxidant =0.25 ml].

The results are plotted in Figures 6-8 respectively. It can be seen that when the time of reaction was raised from (45 to 90 min), the removal of DBT increased from 30.13% to 40.26%, Proceed with an increase in the time of reaction, from (90 - 180 min), the DBT removal efficiency has declined. An increase in reaction time leads to a higher conversion due to a rise in the contact time of the reactants with the active site of the catalyst [23]. On this basis, DBT concentration 385 ppm for modeled oil, time 90 min, and 20%SnO_2/rGO catalyst were employed as constant parameters for further study.

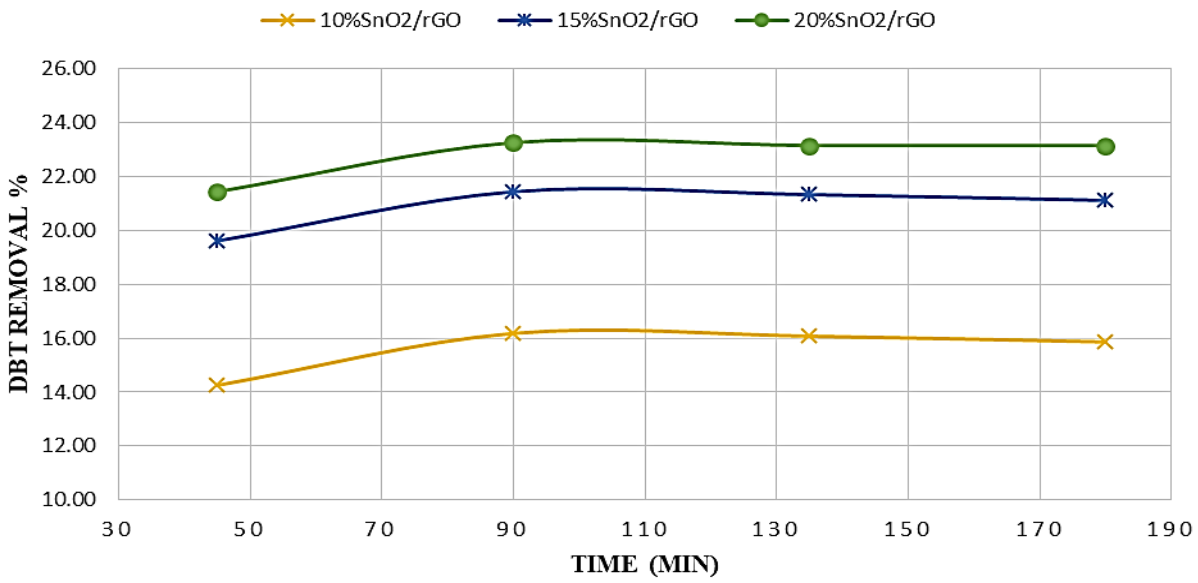

Figure 8. Comparison of the activities of the catalysts at concentration of dibenzothiophene 933 ppm [Reaction conditions: T = 50 ºC, Cat. dos = 0.02 g, and amount of oxidant =0.25 ml].

3.2.2. Effect of Initial Concentrations of DBT

The effect of initial concentrations of DBT on the ODS process was studied at ranging (385 – 933 ppm). The results are plotted in Figure 9, we observe that as DBT concentration was increased from 385 to 933 ppm, the removal of DBT decreased linearly from 40.26 % to 23.26 %, because the number of active sites on the surface of catalyst was insufficient for DBT oxidation at high concentration[24]

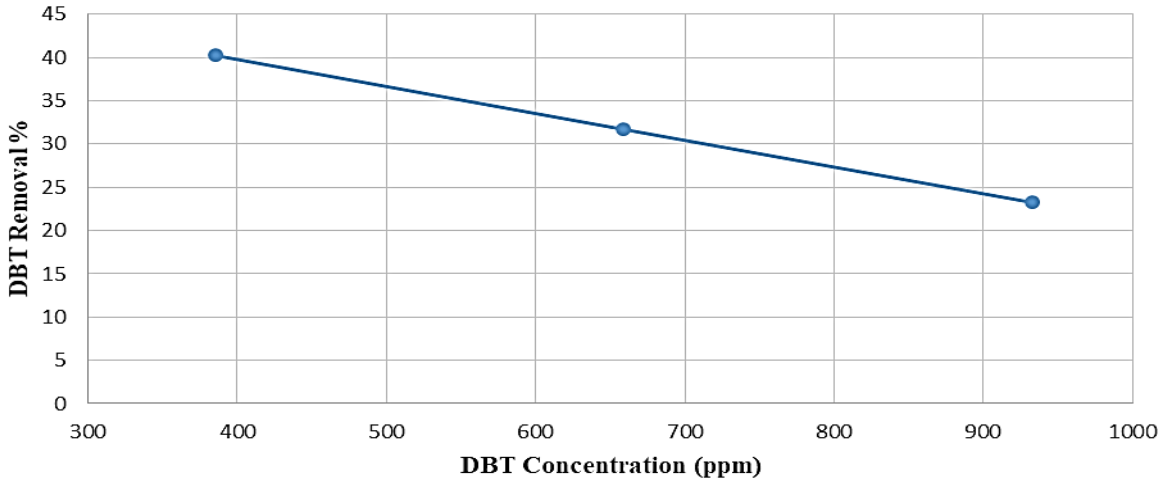

Figure 9. Effect of initial DBT concentration on oxidation reaction at operating conditions [T = 50 ºC, t = 90 min, Cat. dos = 0.02g and amount of oxidant = 0.25 ml]

3.2.3. Effect of Reaction Temperature

DBT removal was studied at a different range of temperatures (40 ◦C to 70 ◦C), while other parameters remained constant. The results were shown in Figure 10, we see that when the temperature is raised from 40 to 60 ◦C the DBT removal increases from 60 % to 79.14 %, due to that the rate of reaction obviously increases when the temperature is increased, whereas above 60 ◦C, DBT removal declines. It has been shown that higher temperatures lead to rapid dissociation of H_2O_2, which leads to a lower DBT removal [25]. These results are in agreement with the literature [26].

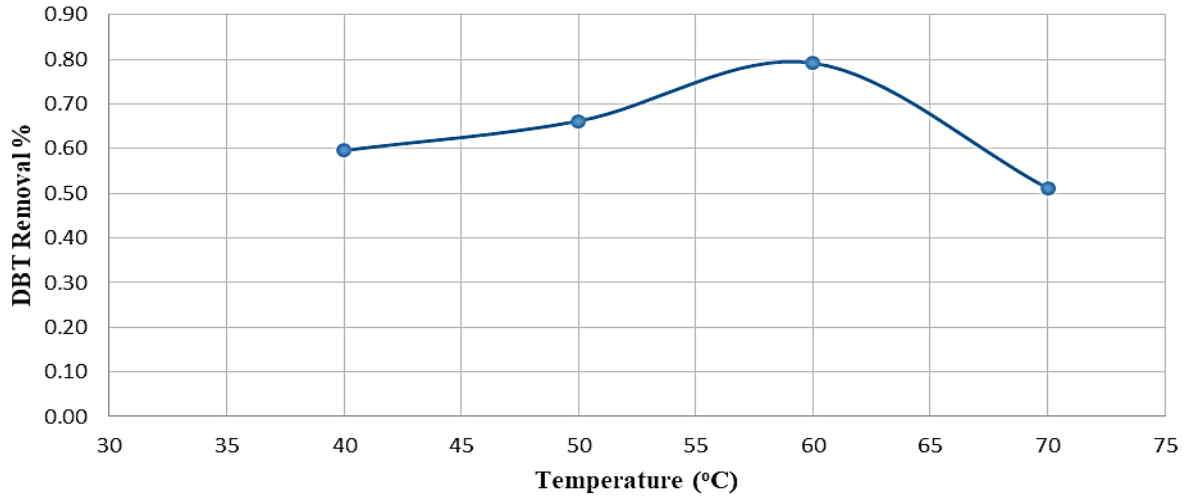

Figure 10. Effect of temperature of reaction on DBT removal

3.2.4. Effect of Catalyst Dosage

The effect of catalyst dosages on the DBT removal was investigated at (0.02, 0.04, 0.06, and 0.08 g) as illustrated in Figure 11. The results show that maximum DBT removal was 79.14 % which is achieved at the catalyst dosage of 0.04g. In spite of increasing the catalyst dosage from 0.06 to 0.08 g, a decline in DBT removal was observed. Increasing the catalyst dosage above the optimum value (0.04g) may result in the agglomeration of active metal, blocking the active sites, resulting in decreased DBT conversion activity [27].

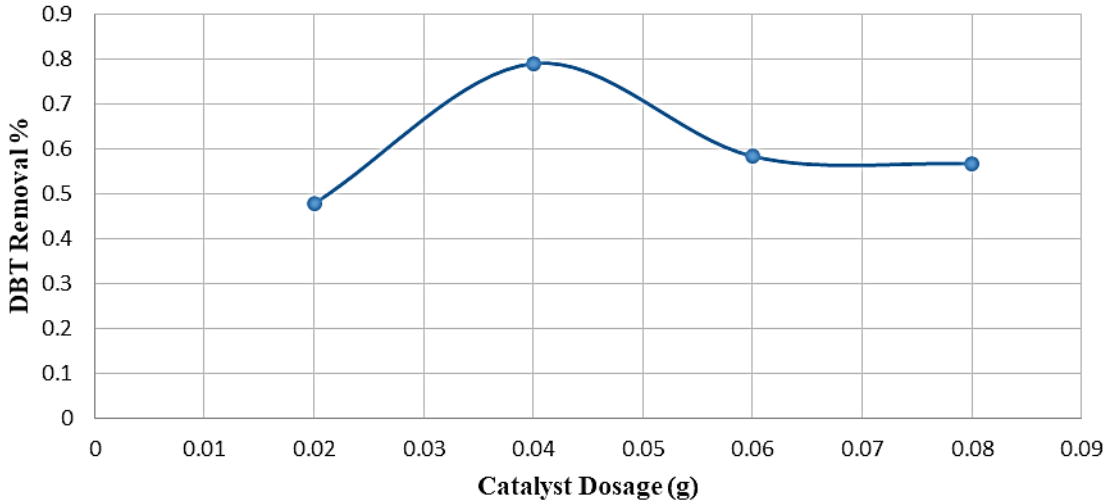

Figure 11. Effect of catalyst dosage on DBT removal

3.2.5. Effect of Amounts of Oxidant

The influence of the different amounts of H_2O_2 in the presence of SnO_2/rGO catalyst was investigated at (0.125, 0.25, 0.375, and 0.5 mL). The experimental data are plotted in Figure 12, and it is shown that the maximum removal of DBT was achieved at 79.14 % when the volume is (0.375 mL). Furthermore, the use of an excessive amount of H_2O_2 has an essential impact on the formation of hydroxyl radicals which caused DBT oxidation promotion. in addition, the DBT removal rate dropped dramatically due to adding H_2O_2 will increasing water in the system which caused decreasing in the oxidation rate[27, 28].

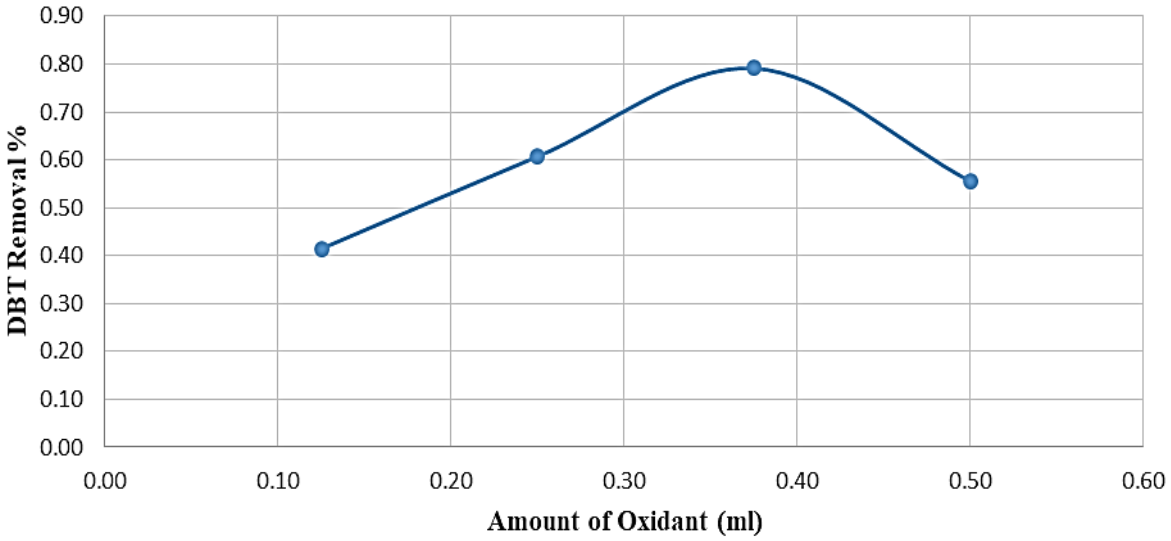

Figure 12. Effect of amount of oxidant on DBT removal

3.4. Kinetic Model for ODS system

Pseudo-first-order and pseudo-second-order kinetic models were used to examine the ODS process using SnO_2/rGO catalyst and H_2O_2 as an oxidizing agent, as shown in equations (2) and (3). From Figure 13a, a linear plot with an R^2 value greater than 0.95 was obtained for a pseudo-first-order kinetic model, indicating that the catalytic ODS reaction follows pseudo-first-order kinetics, while the pseudo-second-order kinetic model has nonlinear relation. Arrhenius formula (Eq. 4) was used to obtain the apparent activation energy of the DBT oxidation reaction and the data is shown in Figure 8b. The activation energy of SnO_2/rGO is 20.34 kJ/mole[29].

$$Ln\frac{C_o}{C_t} = kt \tag{2}$$

$$\frac{1}{C_t} = \frac{1}{C_o} + kt \tag{3}$$

$$Lnk = lnA - \frac{E}{RT} \tag{4}$$

3.5. Reusability of Catalyst

After the ODS reaction is completed, separating the catalyst and recycling it again are essential steps in catalytic technology, that reduce the cost of the process. Thus, after each experiment, the used catalyst was filtered, washed with methanol, and then kept overnight in an oven at 80 °C for drying.

Figure 14 shows the reusability of the catalyst, whereby the removal of DBT decreased slightly from 79.14 to 77 % after three times of use and after eight times DBT removal decreased to 75.5 %.

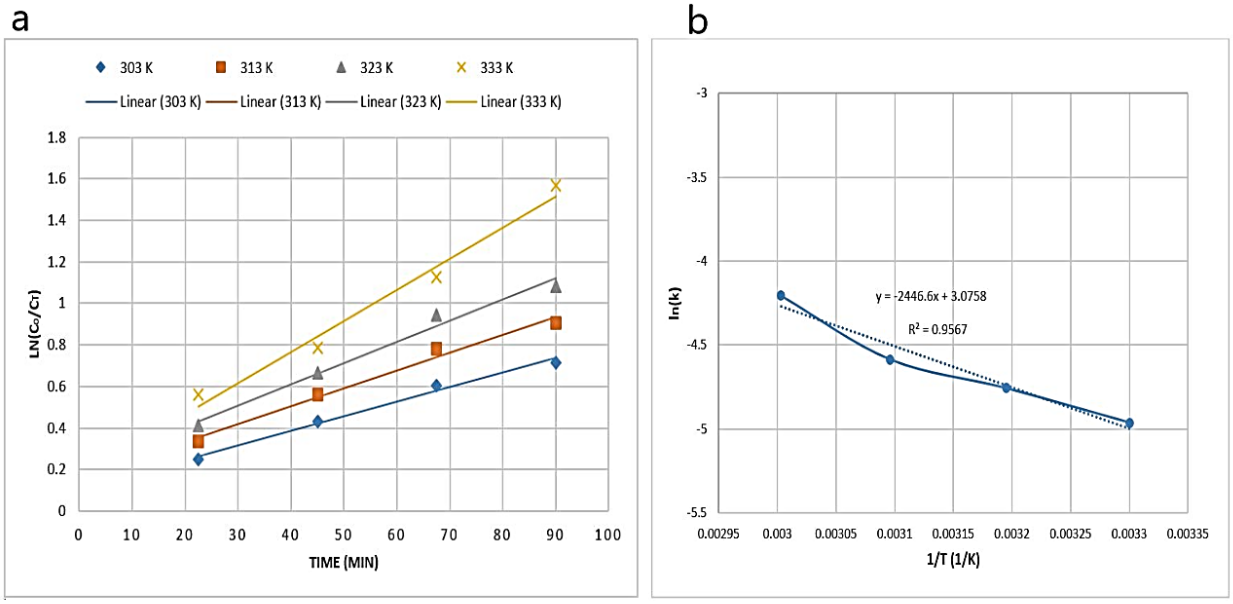

Figure 13. (a) "Pseudo-first-order kinetic model". (b) Activation energies of Arrhenius for ODS process

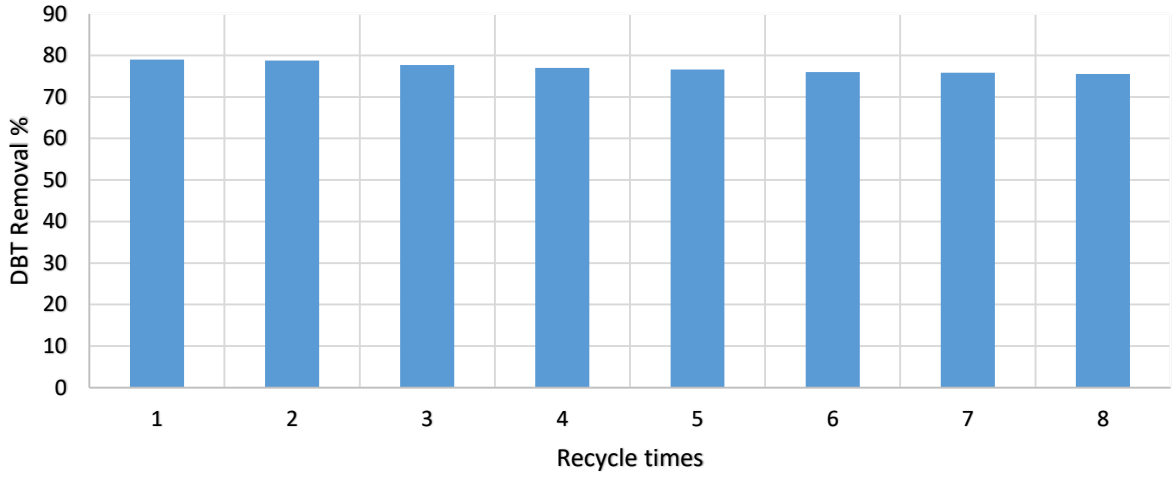

Figure 14. Influence of recycle times on DBT removal.

3.6. Catalytic ODS of Diesel Fuel

The ODS catalyst for diesel fuel with a total sulfur content of 592 ppm was studied under the best conditions for the modeled oil sample (temperature of reaction = 60 ^{o}C, time of reaction = 90 min, catalyst dosage = 0.04 g, amount of H_2O_2 = 0.375 mL). The result showed that the total desulfurization percentage obtained by catalyzed ODS, was 35.81 %.

4. Conclusion

Incipient wetness impregnation (IWI) method was used to prepare SnO_2/rGO catalysts with different Sn loadings (10, 15, and 20 wt. %). The activity of the catalyst towards oxidative desulfurization was evaluated at various operating conditions. The analytical results obtained from XRD, BET, FESEM,

FTIR, and Raman confirm the structure and properties of the composite catalyst. SnO_2/rGO was evaluated in the removal of DBT compounds from simulated diesel fuel using H_2O_2 as an oxidant in a batch reactor. The maximum DBT removal (79.14%) was obtained under the optimum reaction conditions (temperature of reaction = 60 ^oC, time of reaction = 90 min, catalyst dosage = 0.04g, amount of H_2O_2 = 0.375mL, and 385ppm concentration of dibenzothiophene). Catalyst activity at the same operating condition was also investigated for diesel fuel and the removal of sulfur was 35.81%.

Author's Contributions

All authors have read and agreed to the published version of the manuscript.

Competing Interests

The author(s) declare that they have no competing interests.

References

[1]. S. Houda, C. Lancelot, P. Blanchard, L. Poinel, and C. Lamonier, "Oxidative Desulfurization of Heavy Oils with High Sulfur Content: A Review," *Catalysts*, vol. 8, no. 344, pp. 1–26, 2018.

[2]. A. Akopyan, E. Eseva, P. Polikarpova, A. Kedalo, A. Vutolkina, and A. Glotov, "Deep Oxidative Desulfurization of Fuels in the Presence of Brönsted Acidic Polyoxometalate-Based Ionic Liquids," *Molecules*, vol. 25, pp. 1–14, 2020.

[3]. A. Farshi and P. Shiralizadeh, "SULFUR REDUCTION OF HEAVY FUEL OIL BY OXIDATIVE DESULFURIZATION (ODS) METHOD," *Pet. Coal*, vol. 57, no. 3, pp. 295–302, 2015.

[4]. J. M. Campos-Martin, M. C. Capel-Sanchez, P. Perez-Presas, and J. L. G. Fierro, "Oxidative processes of desulfurization of liquid fuels," *J Chem Technol Biotechnol*, vol. 85, pp. 879–890, 2010.

[5]. L. T. Abdulateef, A. T. Nawaf, Q. A. Mahmood, O. S. Dahham, N. Z. Noriman, and Z. Shayfull, "Preparation, characterization and application of alumina nanoparticles with multiple active component for oxidation desulfurization," in *AIP Conference Proceedings*, 2018, vol. 2030.

[6]. Z. Shayegan, M. Razzaghi, A. Niaei, D. Salari, and M. taghi S. Tabar, "Ultrasonic Waves Effect on Oxidative Desulfurization Process of Gas Oil," *14thIranian Natl. Chem. Eng. Congr. (IChEC 2012)*, pp. 1–5, 2012.

[7]. B. N. Bhadra and S. H. Jhung, "Oxidative desulfurization and denitrogenation of fuels using metal-organic framework-based/-derived catalysts," *Appl. Catal. B Environ.*, vol. 259, pp. 1–25, 2019.

[8]. A. S. Ogunlaja, "OXIDATIVE DESULFURIZATION OF FUEL OILS-CATALYTIC OXIDATION AND ADSORPTIVE REMOVAL OF ORGANOSULFUR COMPOUNDS," 2013.

[9]. G. Balkourani, Theodoros Damartzis, A. Brouzgou, and P. Tsiakaras, "Cost Effective Synthesis of Graphene Nanomaterials for Non-Enzymatic Electrochemical Sensors for Glucose: A Comprehensive Review," *sensors*, vol. 22, pp. 1–24, 2022.

[10]. A. T. Smith, A. M. LaChance, S. Zeng, B. Liu, and L. Sun, "Synthesis, properties, and applications of graphene oxide/reduced graphene oxide and their nanocomposites," *Nano Mater. Sci.*, vol. 1, pp. 31–47, 2019.

[11]. N. D. M. Ridzuan, M. S. Shaharun, K. M. Lee, I. U. Din, and and P. Puspitasari, "Influence of Nickel Loading on Reduced Graphene Oxide-Based Nickel Catalysts for the Hydrogenation of Carbon Dioxide to Methane," *Catalysts*, vol. 10, no. 471, pp. 1–15, 2020.

[12]. A. T. Nawaf, S. A. Hameed, L. T. Abdulateef, M. S. K. Aysar T. Jarullah, and I. M. Mujtaba, "A Novel Synthetic Nano-Catalyst (Ag2O3/Zeolite) for High Quality of Light Naphtha by Batch Oxidative Desulfurization Reactor," *Bull. Chem. React. Eng. Catal.*, vol. 16, no. 4, pp.

716–732, 2021.
[13]. S. N. Alam, N. Sharma, and L. Kumar, “Synthesis of Graphene Oxide (GO) by Modified Hummers Method and Its Thermal Reduction to Obtain Reduced Graphene Oxide (rGO),” *Sci. Res. Publ.*, no. 6, pp. 1–18, 2017.
[14]. H. H. Alwan, A. A. Ali, and H. F. Makki, “Optimization of oxidative desulfurization reaction with Fe2O3 catalyst supported on graphene using box-behnken experimental method,” *Bulletin of Chemical Reaction Engineering & Catalysis*, vol. 15, no. 1. pp. 175–185, 2020.
[15]. A. Liu, M. Zhua, and B. Dai, “A novel high-performance SnO2 catalyst for oxidative desulfurization under mild conditions,” *Appl. Catal. A, Gen.*, vol. 583, pp. 1–7, 2019.
[16]. Y. Y. Muhi-Alden and K. A. Saleh, “Removing of Methylene Blue Dye from its Aqueous Solutions Using Polyacrylonitrile/Iron Oxide/Graphene Oxide,” *Iraqi J. Sci.*, vol. 63, no. 6, pp. 2320–2330, 2022.
[17]. Z. Liu *et al.*, “Lateral Size of Graphene Characterized by Atomic Force Microscope,” in *IOP Conf. Series: Earth and Environmental Science*, 2019, pp. 1–6.
[18]. C. A. Zito, T. M. Perfecto, and D. P. Volanti, “Impact of reduced graphene oxide on the ethanol sensing performance of hollow SnO2 nanoparticles under humid atmosphere,” *Sensors Actuators B Chem.*, vol. 244, pp. 466–474, 2017.
[19]. D. López-Díaz, J. A. Delgado-Notario, V. Clericò, E. Diez, M. D. Merchán, and M. M. Velázquez, “Towards Understanding the Raman Spectrum of Graphene Oxide: The Effect of the Chemical Composition,” *Coatings*, vol. 10, no. 524, pp. 1–12, 2020.
[20]. Z. Wei, M. Liu, H. Li, S. Sun, and L. Yang, “SnO2 quantum dots decorated reduced graphene oxide nanosheets composites for electrochemical supercapacitor applications,” *Int. J. Electrochem. Sci.*, vol. 15, pp. 6257–6268, 2020.
[21]. G. Sobon *et al.*, “Graphene Oxide vs. Reduced Graphene Oxide as saturable absorbers for Er-doped passively mode-locked fiber laser,” *Opt. Express*, vol. 20, no. 17, pp. 1–12, 2012.
[22]. W. Ahmad *et al.*, “Oxidative desulfurization of petroleum distillate fractions using manganese dioxide supported on magnetic reduced graphene oxide as catalyst,” *Nanomaterials*, vol. 11, no. 203, pp. 1–16, 2021.
[23]. M. N. Abbas and H. A. Alalwan, “Catalytic Oxidative and Adsorptive Desulfurization of Heavy Naphtha Fraction,” *Korean Chem. Eng. Res*, vol. 57, no. 2, pp. 283–288, 2019.
[24]. Basma Abbas Abdulmajeed, S. Hamadullah, and F. A. Allawi, “Deep Oxidative Desulfurization of Model fuels by Prepared Nano TiO2 with Phosphotungstic acid,” *J. Eng.*, vol. 24, no. 11, pp. 41–52, 2018.
[25]. L. Qiu *et al.*, “Oxidative desulfurization of dibenzothiophene using a catalyst of molybdenum supported on modified medicinal stone,” *RSC Adv.*, vol. 6, pp. 17036–17045, 2016.
[26]. S. S. Otaghsaraei, M. Kazemeini, S. Hasannia, and A. Ekramipooya, “Deep oxidative desulfurization via rGO-immobilized tin oxide nanocatalyst: Experimental and theoretical perspectives,” *Adv. Powder Technol.*, vol. 33, no. 3, p. 103499, 2022.
[27]. S. Sheibani, K. Zare, M. Safavi, and S. Mohammad, “Investigation of Oxidative Desulfurization of Light Naphtha by NiMo/Al2O3 Catalyst,” *Iran. J. Chem. Chem. Eng.*, vol. 40, no. 2, pp. 417–427, 2021.
[28]. W. T. Mohammed, R. F. K. Almilly, and S. B. A. Al-Ali, “Desulfurization of Diesel Fuel by Oxidation and Solvent Extraction,” *J. Eng.*, vol. 21, no. 2, pp. 87–102, 2015.
[29]. P. Huang, G. Luo, L. Kang, M. Zhu, and B. Dai, “Preparation, characterization and catalytic performance of HPW/aEVM catalyst on oxidative desulfurization,” *RSC Adv*, vol. 7, pp. 4681–4687, 2017.